Polymer Journal (2013) 45, 202–209

www.nature.com/pj

ORIGINAL ARTICLE

Self-assembled nanoparticles of PLGA-conjugated glucosamine as a sustained transdermal drug delivery vehicle

Mohana Marimuthu, Devasier Bennet and Sanghyo Kim

Glucosamine (GlcN), an amino-monosaccharide, is known to be a safe and efficient drug for the treatment of various inflammatory diseases, including osteoarthritis and rheumatoid arthritis. In this current study, the main issues of high hydrophilicity and poor permeability of GlcN for its use as a transdermal delivery system were overcome by conjugation with the hydrophobic polymer poly(D,L-lactic-*co*-glycolic acid) (PLGA) and its self-assembly into nanostructures containing nanoparticles (NPs). The self-assembly of the PLGA–GlcN nanostructure was facilitated by probe sonication, which was based on the cavitation and nucleation concept, followed by reversible locking. Hydrophobic PLGA assembly onto the outer surface and hydrophilic GlcN into the inner core helps the nanostructure more flexibly permeate through the skin lipid membrane and release GlcN in a sustained manner for 48 h. *Ex vivo* transdermal permeation of PLGA–GlcN nanostructures through human cadaver skin exhibited a better permeation profile, which demonstrated the shortest lag time with a higher flux value than the other formulations, such as the GlcN solution, GlcN NPs and PLGA–GlcN solution.
Polymer Journal (2013) **45,** 202–209; doi:10.1038/pj.2012.103; published online 13 June 2012

Keywords: conjugation; glucosamine; nanoparticle skin permeation; PLGA; self-assembly; sustained drug delivery

INTRODUCTION

Potential investigations of nanomaterials, especially nanoparticles (NPs), for the efficient delivery of active pharmaceuticals through various administration routes are of great interest to pharmaceutical researchers. NPs for oral and parenteral drug administration have been extensively studied to determine their sustained drug release capability.[1,2] During the last decade, NPs have been examined for prolonged drug release through topical administration for maintaining the drug concentration in the skin for a longer duration. Indeed, some researchers have used sunscreens containing NPs as cream or gel-based formulations for topical administration to protect the skin from ultraviolet exposure for a longer period of time.[3–7] Another example of a successful topical NP drug delivery system is silver NPs.[8] Silver ions were observed to be released slowly from a topical silver NP formulation, which provided prolonged antimicrobial and wound-healing effects in the skin. Rather than using NPs as drug carriers, which may be retained on the skin surface after delivering the drug into skin, utilizing NPs as a delivery vehicle makes them a successful transdermal candidate for prolonged drug delivery.[9] Some examples of drug delivery vehicles are liposomes, polymeric NPs, and so on, which are designed to maintain the physicochemical properties of the encapsulated drugs and facilitate drug delivery.[10,11]

For decades, the self-assembly of complex nanostructures from simple colloidal NPs has been of practical interest for building materials with unique properties for use as drug delivery carriers. Self-assembly is the process of inter- and intra-molecular bonding through van der Waals forces or hydrophobic interactions, which normally results in close-packed structures. These close-packed structures may be either colloidal crystals or particle clusters, depending on where the assembly process occurs, such as in the bulk fluid[12] or in the liquid–liquid interface,[13] respectively. Polymer-based self-assembled nanostructures are one of the potential nano vehicles for delivering a wide range of pharmaceutical agents. Because of their good biocompatibility and natural degradation/resorption pathways, some polymers, such as poly(lactic acid), poly(glycolic acid) and poly(D,L-lactic-*co*-glycolic acid) (PLGA), in the form of NPs have been extensively studied for use as drug delivery carriers.[14] Several studies on NP-based oral and parenteral formulations of PLGA were studied, and because of their high stability they were found to be more advantageous than liposomes.[15–17] There are reports on the efficiency of PLGA-based nanoformulations for the transdermal delivery of drugs, such as flufenamic acid, and bioactive agents, such as plasmid DNA.[18,19]

GlcN hydrochloride, an amino sugar abundantly found in the articular cartilage matrix, has been studied extensively for the

Department of Bionanotechnology, Gachon University, Seoul, Republic of Korea
Correspondence: Dr S Kim, Department of Bionanotechnology, Gachon University, San 65, Bokjeong dong, Seoul 461701, Republic of Korea.
E-mail: samkim@gachon.ac.kr
Received 29 December 2011; revised 22 March 2012; accepted 9 April 2012; published online 13 June 2012

treatment of osteoarthritis. Commercially available GlcN is mainly administered orally, which causes gastric irritation and ulcers when used over the long term. In addition, GlcN undergoes extensive hepatic first-pass metabolism and, therefore, the oral form has very low bioavailability.[20] These difficulties make the transdermal delivery of GlcN the best alternative route of administration, although the high water solubility and absorption parameters are limitations for designing skin permeation formulations.[21]

Therefore, in this study, the high aqueous solubility of GlcN was reduced by cross-linking with PLGA (PLGA–GlcN), a lipophilic polymer, and then self-assembling into NP nanostructures. The current work utilized probe sonication to synergistically catalyze the self-assembly of nanostructures from colloidal NPs of the conjugated PLGA–GlcN polymer. The conjugated polymer PLGA–GlcN-based self-assembled nanostructures were evaluated for transdermal GlcN delivery as a drug and were then compared with other GlcN formulations. Several drug permeation parameters were derived from the permeation micrographs.

EXPERIMENTAL PROCEDURE

Materials

Poly(D,L-lactic-*co*-glycolic acid) acid terminated (PLGA; 50:50), GlcN hydrochloride, 4-dimethylaminopyridine, 1-ethyl-3-(3-dimethyl aminopropyl) carbodiimide (EDC), polyvinyl alcohol (M_w 130 000), phosphate-buffered saline tablets, and dimethyl sulfoxide (99.9% purity and cell culture tested) were purchased from the Sigma-Aldrich Chemical Co. Ltd. (Seoul, South Korea). Diethyl ether (99% purity) was obtained from the Junsei Chemical Co. Ltd, Tokyo, Japan. All chemicals and solvents used in this work were of analytical grade.

The molecular weight of the PLGA is 17 000 with a polydispersity index of 1.5 ± 0.1, inherent viscosity of 0.16–0.24 dl g^{-1} and a minimum acid value of 6 mg KOH per gram.

Conjugation of PLGA and GlcN

The chemical conjugation of the PLGA–GlcN was performed using an EDC system.[22] Briefly, PLGA (0.5 g, 1.5 mM) and 4-dimethylaminopyridine (0.047 g, 0.02 M) were dissolved in 18 ml of dimethyl sulfoxide by ultrasonication. The solutions were then mixed with 1 ml of GlcN solution (1 g, 0.25 M in deionized water). The GlcN solution was added dropwise to the PLGA/4-dimethylaminopyridine solution, followed by the addition of the EDC solution (0.55 g, 0.1 M in 2 ml of dimethyl sulfoxide) and then maintained at room temperature for 3 h. Then, the mixed solution was poured into an excess of acetone to produce the precipitate. The precipitate was filtered and dissolved in distilled water. As PLGA is insoluble in water, the undissolved and unconjugated PLGA was separated from the PLGA–GlcN solution. The unconjugated GlcN in the PLGA–GlcN solution was removed by dialyzing with a semi-permeable membrane (dialysis bag) for two days. Finally, the purified sample was lyophilized until dry and then stored. The percentage yield was found to be 97.1%.

Fourier transform infrared analysis and nuclear magnetic resonance analysis

The Fourier transform infrared (FT-IR) spectra for free GlcN, free PLGA, and conjugated PLGA–GlcN were obtained using a TENSOR 27 spectrophotometer (Bruker Optics Co. Ltd., Seoul, South Korea) for analyzing the chemical modifications after conjugation of PLGA with GlcN. The spectra were obtained between 4000–500 cm^{-1}.

Nuclear magnetic resonance (NMR) spectra were recorded on a 400 MHz ^1H NMR spectrometer (AVANCE 400 WB, Bruker BioSpin Co. Ltd., Seoul, South Korea) using a commercially available deuterated solvent (D_2O). The proton chemical shifts are reported in parts per million (p.p.m., δ).

Preparation of PLGA–GlcN NPs

PLGA–GlcN (7.5%) and polyvinyl alcohol (5%) were mixed in 1 ml of DI H_2O. The above mixture was added dropwise to 3 ml of diethyl ether under probe sonication for 5 min to form a w/o emulsion. Simultaneously, 1 ml of 1% Tween-20 was mixed with 9 ml of ethanol. The above formed w/o emulsion mixture was then added dropwise to the Tween-20/ethanol solution, and sonication was continued for 2 min. Finally, the mixture was mixed using a magnetic stirrer at 1200 r.p.m. for 2 h. This w/o/w emulsion of a milky white solution contains the self-assembled raspberry-like PLGA–GlcN nanostructure. The nanostructure was then centrifuged, separated, dried and stored for further experiments.

Preparation of GlcN NPs

The procedure for preparing the PLGA–GlcN NPs was followed, except that 5% of GlcN hydrochloride powder was used instead of the PLGA–GlcN samples.

Preparation of the GlcN solution

The required quantity of GlcN was dissolved into distilled water to prepare a 5% concentration of the GlcN solution.

Preparation of the PLGA–GlcN solution

The required quantity of conjugated PLGA–GlcN was dissolved into distilled water to prepare a 7.5% concentration of a PLGA–GlcN solution that contained 5% GlcN.

Characterization

FE-SEM analysis. The surface morphologies of the synthesized PLGA–GlcN NPs and GlcN NPs were characterized using a field emission scanning electron microscope (FE-SEM; JEOL-ISM-7500F, JEOL Korea Ltd., Seoul, South Korea). A single drop of the emulsion was placed onto a pre-cleaned glass cover slip, air dried and then sputter-coated with platinum before being visualized using the FE-SEM.

Dynamic light scattering. The particle size distribution and zeta potential of the PLGA–GlcN nanostructures and the GlcN NPs were determined using a Malvern Zetasizer Nano ZS Series (Malvern Instruments Korea, Seoul, South Korea), with a 633-nm laser and a scattering angle of 90°.

In vitro skin permeation study. The human cadaver skin samples with a size of 3 cm^2 were obtained from the Hans Biomed Corp., Seoul, Korea and stored at −20 °C. A Franz-Diffusion cell, with an effective diffusion area of 1.72 cm^2, was used to carefully mount the skin samples to position the stratum corneum layer facing up. Then, 15 ml of phosphate-buffered saline (pH 7.4) was added to the receptor compartment, and the donor compartment was filled with various drug preparations (GlcN solution, PLGA–GlcN solution, GlcN NPs, PLGA–GlcN NPs). All of the preparations were adjusted to a GlcN concentration of 5% for every experiment. The entire setup was kept in an immersed condition and maintained at 37 ± 0.5 °C with magnetic stirring at 100 r.p.m. throughout the experiment. At different time intervals (0, 1, 2, 3, 6, 12, 18, 24, 30, 36, 42 and 48 h), 1 ml of sample was withdrawn from the receptor compartment and replaced with fresh phosphate-buffered saline solution. Then, the samples were analyzed with a ultraviolet–visible spectrophotometer (Optizen 3220, Mecasys Co. Ltd., Daejeon, South Korea) at a wavelength of 250 nm for their GlcN content after derivatization into phenylthiocarbamyl–GlcN using phenyl isothio-cyanate as a derivatization reagent, following the procedure given by Tekko *et al.*[20]

Statistical analysis. Statistical analysis was performed with the GraphPad Prism 5 software (GraphPad Software, Inc., La Jolla, CA, USA) using the one-way ANOVA followed by the Tukey multiple comparison test. The data were considered to be significant at $P < 0.05$.

RESULTS

FT-IR analysis of PLGA–GlcN

The PLGA was conjugated to GlcN using the basic principle developed by Murakami *et al.*,[22] who have cross-linked poly (γ-glutamic acid) with several saccharides. The present group utilized EDC for activating the carboxylic group of PLGA. The hydroxyl group of GlcN was then attached to the EDC-activated

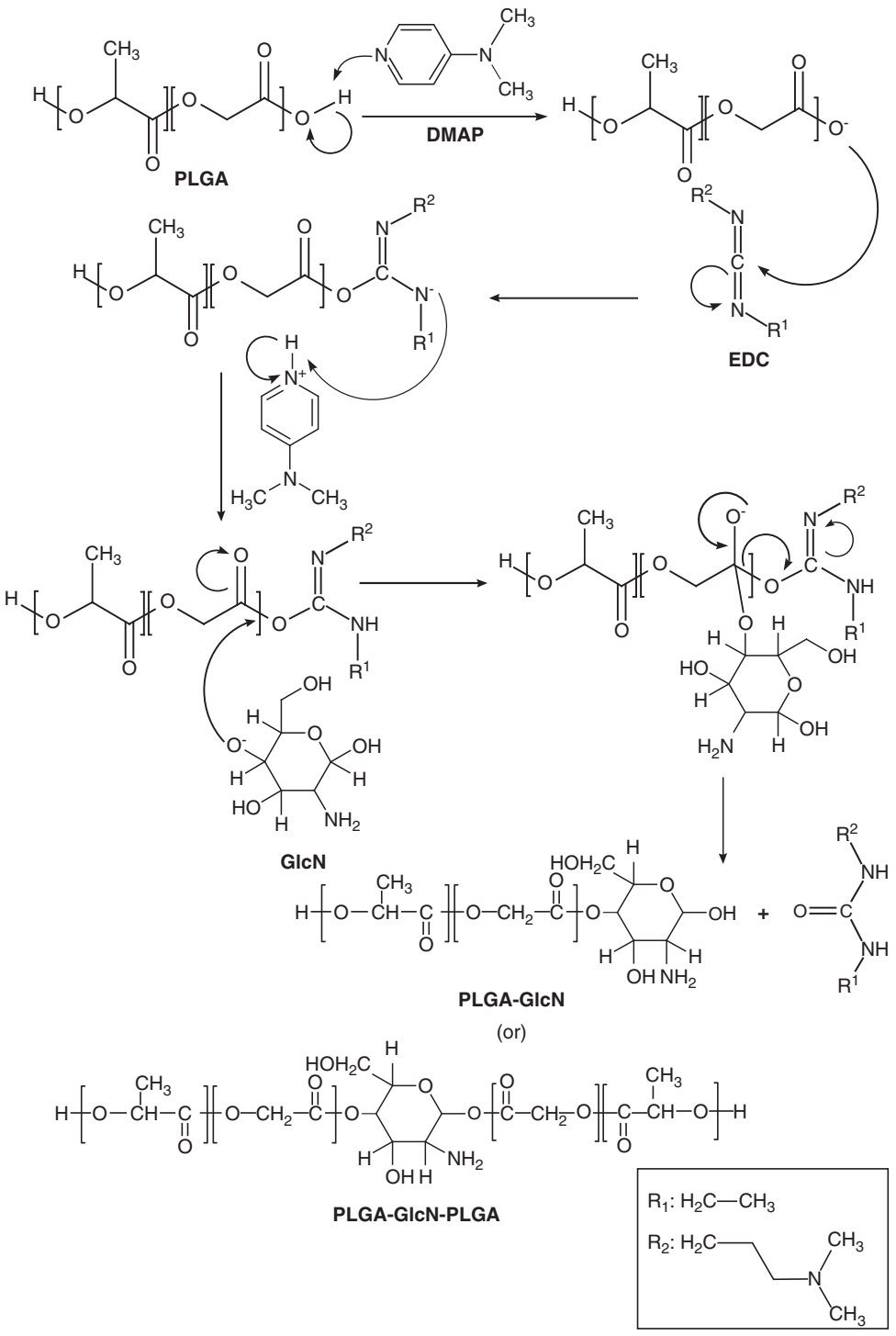

Figure 1 Chemical conjugation of PLGA with GlcN using an EDC-based system.

carboxylic acid group of PLGA. The reaction scheme was shown in Figure 1. A recovery yield of 55.2% and a grafting yield of 41.3% were obtained for GlcN. The FT-IR spectral analysis was used to confirm the successful conjugation of PLGA with GlcN. The FT-IR spectra of GlcN, PLGA and the PLGA–GlcN were shown in Figure 2. The -NH_2 bending peaks at $\sim$1600 cm^{-1} and a doublet peak at 3290 cm^{-1} for the -NH_2 group of the primary amine were observed in the spectra for both GlcN and PLGA–GlcN.[23] This result confirms that the free -NH_2 group of GlcN remains after conjugating with PLGA. As the medicinal property of GlcN is chemically dependent on the presence of its -NH_2 group,[24,25] it is important to ensure that the PLGA–GlcN conjugation did not occur on the -NH_2 group. A peak at 2948 cm^{-1} that was over 500 cm^{-1} wide and a strong peak at 1759 cm^{-1} were observed in the PLGA spectrum and result from the carboxylic O–H and carboxylic C=O groups, respectively.[26] The absence of these peaks in the conjugated PLGA–GlcN spectrum confirms that the -COOH group of PLGA was modified and utilized for conjugating with the terminal -OH group of GlcN, as shown in Figure 1. The peak

at 1705 cm^{-1} in the PLGA–GlcN spectrum was due to the carbonyl C = O stretch of the ester linkage. Owing to the presence of another carbonyl group (from the polylactide group of PLGA) near the C = O of the ester linkage with GlcN, the absorption was lowered by ~50 cm^{-1} from 1759 cm^{-1}, which corresponds to the carboxylic C = O group in PLGA, to 1705 cm^{-1} in PLGA–GlcN.[26] A broad peak at 3500 cm^{-1}, corresponding to the alcoholic O–H group of PLGA, appeared after conjugation with GlcN and was similar to the peak at 3520 cm^{-1} in the PLGA spectrum. The multi-banded peak at ~2800 cm^{-1} in the PLGA–GlcN spectrum arises from the C–H of the sp^3 carbon in PLGA.[26] Furthermore, in the PLGA–GlcN spectrum, peaks from GlcN, such as 1092 and 1030 cm^{-1} for the -CN stretch and the primary alcohol -C–O stretch, respectively, appeared in addition to the peaks from PLGA.[26] This observation proved that the PLGA conjugated with the GlcN moieties.

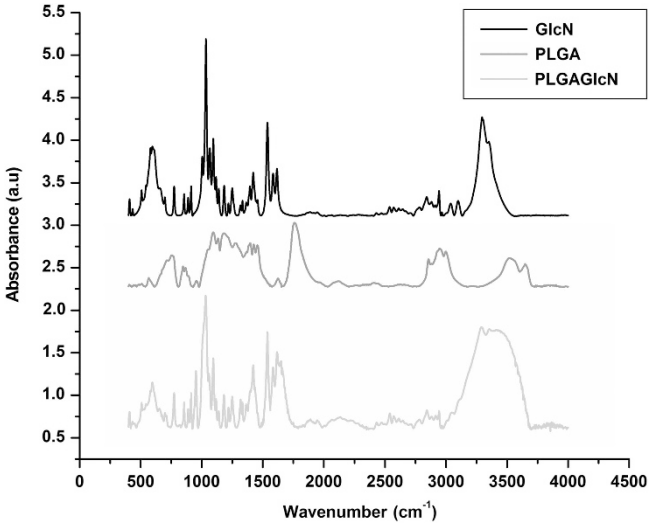

Figure 2 FT-IR spectrum of PLGA, GlcN and conjugated PLGA–GlcN. A full color version of this figure is available at *Polymer Journal* online.

NMR analysis of PLGA–GlcN

Figure 3 shows the ^1H NMR chemical shifts of the conjugated PLGA–GlcN polymer. The chemical shifts at 1.07–1.21 p.p.m. were assigned to the sp^3-hybridized C–H protons of PLGA (Figure 3a).[27] The triplet at 1.9 p.p.m. corresponds to the proton of CH_2 that is close to the carboxyl group (Figure 3c).[28] The proton shifts at 2.61 p.p.m. were due to the CH that is associated with methyl and carboxylic ester (Figure 3b).[29] The GlcN containing CH proton near the amine group presents a chemical shift at 2.73 p.p.m. (Figure 3f).[30] The resonance from 2.84 p.p.m. to 3.96 p.p.m. was obtained; these signals normally appear when the sp^3-hybridized C–H is attached to double-bonded functional groups, such as esters or ketones.[29] According to the present research, these resonance shifts correspond to the protons of the oxygenated sp^3 C–Hs that have ester linkages after the conjugation of PLGA–GlcN. The proton shifts at 3.29–3.32 p.p.m. were the result of the CH_2 proton that was bonded to the GlcN OH group (Figure 3e).[29] In addition, a doublet proton shift at 3.77 p.p.m. was observed, which corresponds to the CH that is attached to the acetylated hydroxyl group of GlcN, which further confirms the successful conjugation of PLGA with GlcN at the C_4 or C_1 position (Figure 3d).[31] The proton shift at 4.95 p.p.m. was due to the polyglycolide methylene proton of PLGA.[29] Furthermore, the spectrum presents a peak at 5.45 p.p.m. that arises from the polylactide methyl proton of PLGA.[29] The chemical shift at 8.75 p.p.m. (Figure 3g) confirms the presence of the amine NH proton.[28,32] The resonance of this amine proton was weak because the addition of D_2O causes all of the hydrogen on the non-carbon atoms to exchange with deuterium. In addition, the absence of a broad singlet peak at higher resonance corresponding to the carboxylic acid hydrogen of PLGA, and the presence of a signal for the ester linkage proves the successful conjugation of PLGA with GlcN.

Characterization of GlcN NPs and PLGA–GlcN NPs

Monodispersed GlcN NPs with a smooth surface morphology were obtained, as shown in the FE-SEM images in Figures 4 a and b. The size analysis of the GlcN NPs showed that the average NP size was 75 ± 25 nm with a zeta potential of 24 ± 1.2 mV (Figure 4c). The

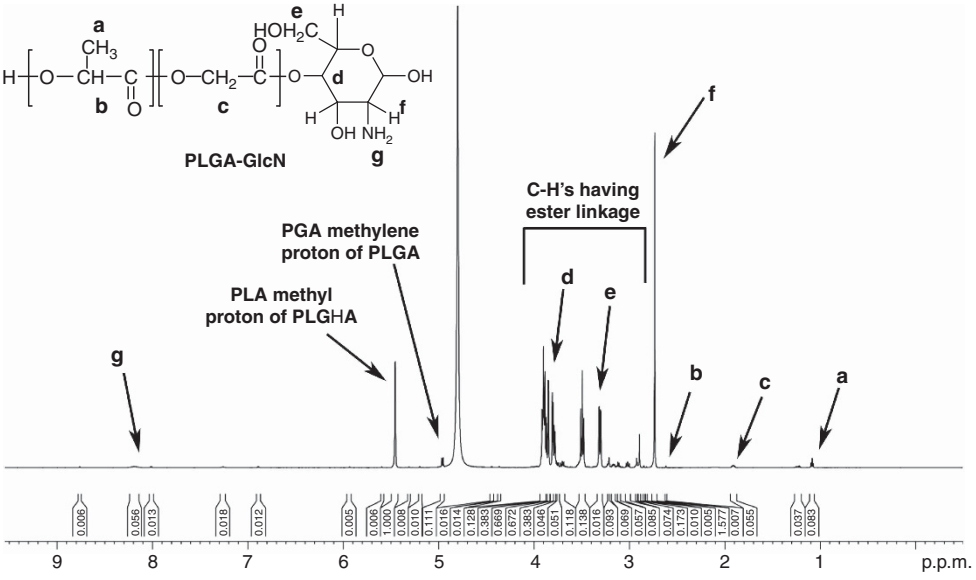

Figure 3 ^1H NMR proton shifts of the conjugated PLGA–GlcN.

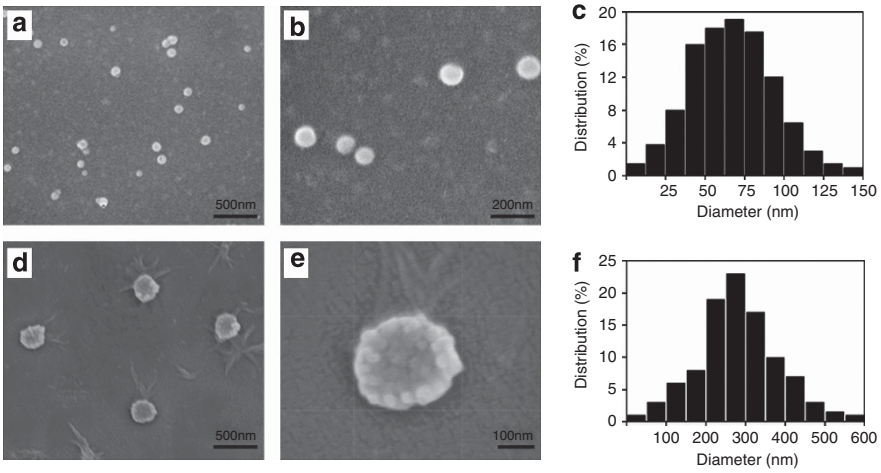

Figure 4 FE-SEM images and size analysis of the GlcN NPs (**a**), (**b**) and **c**, respectively) and the PLGA–GlcN NPs (**d**), (**e**) and (**f**), respectively).

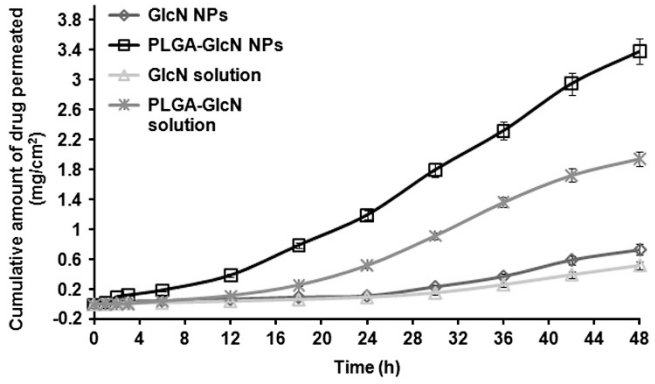

Figure 5 Transdermal permeation profiles of various GlcN formulations.

Table 1 Several permeation parameters of GlcN formulations

	GlcN formulations			
Permeation parameters	*GlcN solution*	*GlcN NPs*	*PLGA–GlcN solution*	*PLGA–GlcN NPs*
Steady-state flux (J_{ss}) ($\mu g\,h^{-1}\,cm^{-2}$)	9.48	13.31	41.19	70.04
Lag time (T_L) (h)	4.51	4.49	3.85	2.72
Permeability coefficient (K_p) ($10^{-3}\,cm^{-1}\,h^{-1}$)	1.89	2.66	8.24	14.01

Abbreviations: GlcN, Glucosamine; NP, nanoparticle; PLGA, poly(D,L-lactic-*co*-glycolic acid).

presented work has utilized sonication to synergize the self-assembly of nanostructures from colloidal NPs of the biologically inspired polymer composite, PLGA–GlcN. Probe sonication at low frequency (20–100 kHz) with an output of 50 W aids in accelerating the reaction kinetics by producing high-energy cavitational bubbles or micro-droplets.[33,34] This method successfully induces the self-assembly of 20 ± 5 nm sized PLGA–GlcN NPs, resulting in a nanostructure with a final size of 250 ± 50 nm and a zeta potential of 18.5 ± 2.1 mV, as determined using the dynamic light scattering technique, and with a raspberry-like morphology, as shown in the FE-SEM image (Figures 4 d–f).

In vitro skin permeation study

The permeation profiles of various GlcN formulations were obtained by plotting the cumulative amount of GlcN that was permeated across a unit area of human cadaver skin against time in hours and are shown in Figure 5. The transdermal delivery potential of various GlcN formulations was studied by calculating some important permeation parameters, such as the steady state flux (J_{ss}), lag time (t_L), and permeability coefficient (K_p). The slope of the linear portion of the permeation profile in Figure 5 gives the J_{ss} values for the respective formulations. Similarly, the t_L values of every formulation were determined from the *x*-intercept of the back extrapolated linear portions.

$$J_{ss} = (dQ/dt)_{ss}.1/A$$

Where Q is the cumulative transdermal drug content, dQ/dt is the rate of change of Q with respect to time (t), and A is the effective diffusion area. The analysis of the linear regression fit to the curve 'Q' vs 't' helps to obtain the slope, dQ/dt.

Finally, the K_p values were calculated using the following formula.

$$K_p = J_{ss}/C_d$$

Here, C_d is the concentration of drug, which remains constant in the vehicle. Table 1 provides the calculated J_{ss}, t_L and K_p values for all GlcN formulations.[35]

DISCUSSION

Exogenous GlcN has been supplied as a safe, over-the-counter drug for inflammatory diseases, such as osteoarthritis and other related ailments, exceeding 700 million dollars in annual sales in the United States alone, according to a survey in 2008.[36] GlcN stimulates the production of proteoglycan and glycosaminoglycan in articular cartilage, which is the most important factor influencing arthritis-type inflammatory diseases.[20] Until the invention of transdermal GlcN cream by the Jonathan Obaje group in 2003,[37] the most popular dosage forms of GlcN commercially available were tablets, capsules, powders and liquids. In some countries, such as Europe,

injectable (intramuscular and intravenous) formulations are also available. As GlcN is acidic, the long-term use of its oral formulations produces gastric irritation and ulcers in some cases. In addition, GlcN is highly prone to hepatic first-pass metabolism, resulting in very low bioavailability.[20] Because of its poor bioavailability, repeated administration of GlcN is needed, which is often inconvenient for patients. An alternative formulation to increase patient compliance would be the transdermal delivery system. As GlcN is highly hydrophilic, it exhibits poor skin permeability, which results in difficulties in formulating a transdermal delivery system. A variety of approaches have been examined for GlcN transdermal delivery formulations, including o/w cream, liposome suspensions, liposomal gel and liquid crystalline vehicles.[35] A recent study showed increased GlcN skin permeation by utilizing oleic acid and polyethylene glycol 200.[35]

Nanomaterial-based transdermal drug delivery carriers have been extensively studied because of their prolonged drug release and maintenance of desired drug concentration.[18,38,39] In particular, PLGA polymer-based NPs, which are biocompatible and biodegradable, have been extensively investigated as transdermal drug carriers during the last decade.[18,19,40] As PLGA is hydrophobic, the present research utilized this characteristic of PLGA to modify the hydrophilic property of GlcN by the chemical conjugation method. It is known that the amino group of GlcN bears therapeutic activity, which is acetylated and activated for the biosynthesis of proteoglycans and glucosaminoglycan in hexosamine biosynthetic pathway.[24,25] Therefore, the PLGA–GlcN conjugation was performed by the esterification of the PLGA's carboxylic acid group with the terminal alcoholic group of GlcN without affecting the GlcN's amino group, as shown in Figure 1. In addition, the resulting PLGA–GlcN contained both the hydrophilic and hydrophobic moieties, thereby overcoming the skin permeation issues due to the high hydrophilicity of GlcN. The FT-IR and NMR results confirm the presence of the -NH_2 and ester groups, and the absence of the carboxylic acid group after the conjugation of PLGA–GlcN.

To produce an efficient, sustainable transdermal GlcN delivery vehicle, this study attempted to synthesize a nanostructure comprised of PLGA–GlcN NPs. For the synthesis of these nanostructures, sonication was utilized to synergistically activate the self-assembly of hydrophilic GlcN into the inner core and hydrophobic PLGA onto the outside of the nanostructure, as shown in Figure 6. Instead of mechanical or magnetic stirring, probe sonication was used for the continuous mixing and accelerated nucleation of PLGA–GlcN.[33] During the dropwise addition of PLGA–GlcN to a non-polar solvent, diethyl ether, under continuous shearing by sonication, the hydrophobic PLGA moiety assembled onto the w/o interface to minimize the total surface energy (Figure 6). Continuous sonication catalyzes the nucleation and subsequent reversible locking of PLGA by van der Waals forces on the outer surface, and similarly, GlcN nucleation on the inner core.[41] Furthermore, the dropwise addition of this solution to the secondary water phase (ethanol) leads to the close-packed arrangement of PLGA and GlcN moieties in a colloidal NP assembly of complex PLGA–GlcN nanostructures (w/o/w emulsion) (Figure 6). Figure 6 illustrates the formation of a closely packed structure. The dropwise addition of the w/o emulsion containing PLGA–GlcN clusters into ethanol under sonication catalyzes the internal locking of PLGA because of a change in surface energy. This process helps in forming a particle-like assembly of PLGA on the outer side of each of the nanostructures. This particle-like assembly on the outer surface of each nanostructure was clearly observed in the FE-SEM images (Figures 4 d and e). As ethanol is known for its excellent membrane permeation, it has been used as a secondary water phase in this current study. It is believed that PLGA–GlcN is self-assembled into a two-dimensional network at the w/o interface, and during the evaporation/drying process, they reversibly buckled to form a densely packed nanostructure.[42,43] The FE-SEM image shown in Figure 4 supports the close-packed structure of PLGA–GlcN nanostructure.

Hydrophobic PLGA facing outside of the nanostructure facilitates the transdermal permeation, and the nanostructure containing GlcN

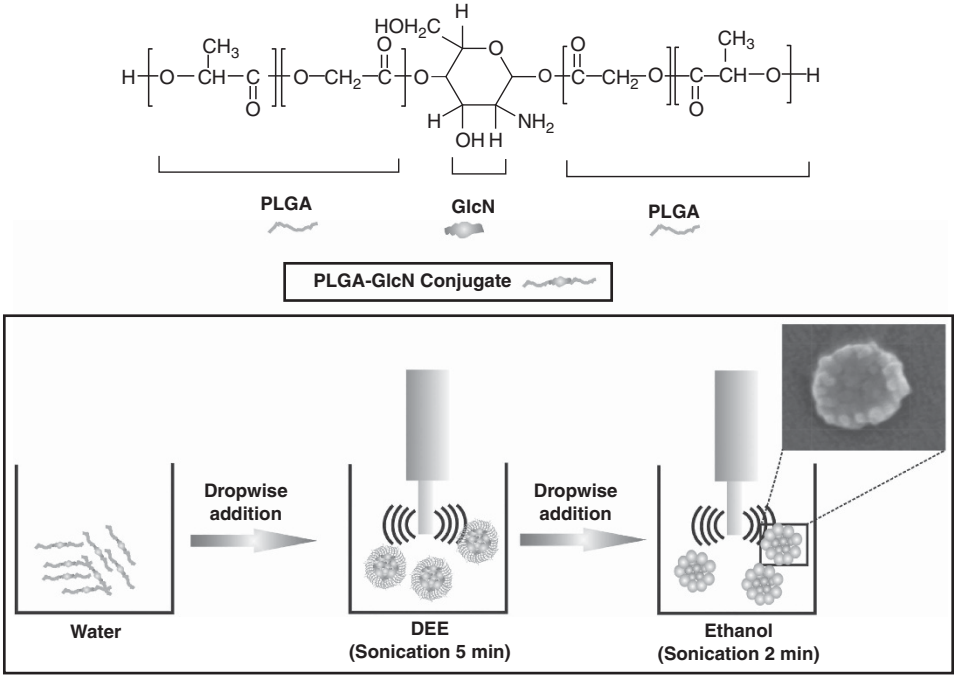

Figure 6 Schematic illustration of sonication assisted self-assembly of the PLGA–GlcN conjugate. A full color version of this figure is available at *Polymer Journal* online.

as the inner core helps the sustained delivery of GlcN. For comparison, several GlcN formulations, including a GlcN solution, GlcN NPs and a PLGA–GlcN solution, were prepared and investigated with the PLGA–GlcN nanostructure for transdermal GlcN delivery (Figure 5). Though the GlcN was formulated as a NP, its permeation profile was more similar to the GlcN solution. Both the GlcN NPs and the GlcN solution permeated very low concentrations of GlcN, such as 0.7 and 0.5 mg cm^{-2}, respectively. As GlcN is highly hydrophilic resulting in poor permeability, these obtained results were in agreement with previous reports.[35] On the basis of the results shown in Figure 5, a significant number of PLGA–GlcN NPs permeated across the human cadaver skin and delivered a high concentration (3.3 mg cm^{-2}) of GlcN compared with the other formulations. This observation may likely be due to its structural similarity to the skin biomembrane.[44–46] The skin biomembrane is a selective barrier, which consists of a lipid bilayer with embedded proteins within or enclosing every cell in the skin tissue. This biomembrane has the essential property of selective permeability for molecules trying to pass through it. The aim of this present research was to enhance the permeability of NPs through the skin tissue by overcoming this barrier layer. Therefore, the NPs with a hydrophobic outer surface and a hydrophilic inner surface resemble the lipid bilayer, which has structural similarity to the skin biomembrane. Because of this structural similarity, the permeation of particles has been enhanced because of minimal rejection by the biomembrane. It is believed that the synthesized particle can adjust its structure with a highly flexibility; in addition, the outer layered hydrophobic PLGA permeates across the lipophilic bilayer of skin through trans-epidermal route, similar to transferosome.[47-50] After the breakdown of PLGA–GlcN from the degradation process, a sustained GlcN release was obtained.[51] The permeation of the PLGA–GlcN solution was lower than that of its NP formulation (1.9 mg cm^{-2} of GlcN), and indeed, they showed a much better permeation profile than the GlcN formulations. This result could be due to the absence of its flexibility in hydrophobic and hydrophilic environments, according to the lipidic bilayer because they are not self-assembled. These results are further supported by the analytical reports of the permeation parameters, as shown in Table 1. Enhanced transdermal GlcN delivery behavior of PLGA–GlcN NPs with a 70 μg h^{-1} cm^{-2} flux value in a shortest lag time of 2.72 h was obtained, which was a much better result than the other GlcN formulations. Furthermore, this new drug formulation has the ability to treat inflammatory diseases such as osteoarthritis, rheumatoid arthritis and other related ailments with high patient compliance because the system can limit repeated drug administration due to its sustained drug release property.

ACKNOWLEDGEMENTS

This research was supported by the Gachon University Research Fund in 2012 (KWU 2011-R274).

1 de Jalon, E. G., Blanco-Prieto, M. J., Ygartua, P. & Santoyo, S. PLGA microparticles: possible vehicles for topical drug delivery. *Int. J. Pharm.* **226,** 181–184 (2001).
2 Jenning, V., Gysler, A., Schafer-Korting, M. & Gohla, S. H. Vitamin A loaded solid lipid nanoparticles for topical use: occlusive properties and drug targeting to the upper skin. *Eur. J. Pharm. Biopharm.* **49,** 211–218 (2000).
3 Nohynek, G. J., Lademann, J., Ribaud, C. & Roberts, M. S. Grey goo on the skin? Nanotechnology, cosmetic and sunscreen safety. *Crit. Rev. Toxicol.* **37,** 251–277 (2007).
4 Filipe, P., Silva, J. N., Silva, R., de Castro, J. L. C., Gomes, M. M., Alves, L. C., Santus, R. & Pinheiro, T. Stratum corneum is an effective barrier to TiO2 and ZnO nanoparticle percutaneous absorption. *Skin Pharmacol. Physiol.* **229,** 266–275 (2009).
5 Hayden, C. G., Roberts, M. S. & Benson, H. A. Systemic absorption of sunscreen after topical application. *Lancet* **350,** 863–864 (1997).
6 Kuo, T. R., Wu, C. L., Hsu, C. T., Lo, W., Chiang, S. J., Lin, S. J., Dong, C. Y. & Chen, C. C. Chemical enhancer induced changes in the mechanisms of transdermal delivery of zinc oxide nanoparticles. *Biomaterials* **30,** 3002–3008 (2009).
7 Szikszai, Z., Kertesz, Z., Bodnar, E., Major, I., Borbiro, I., Kiss, A. Z. & Hunyadi, J. Nuclear microprobe investigation of the penetration of ultrafine zinc oxide into intact and tape-stripped human skin. *Nucl. Instrum. Meth. B* **268,** 2160–2163 (2010).
8 Tian, J., Wong, K. K., Ho, C. M., Lok, C. N., Yu, W. Y., Che, C. M., Chiu, J. F. & Tam, P. K. Topical delivery of silver nanoparticles promotes wound healing. *ChemMedChem* **2,** 129–136 (2007).
9 Hoffman, A. & Ziv, E. Pharmokinetic considerations of new insulin formulations and routes of administration. *Clin. Pharmacokinet.* **33,** 285–301 (1997).
10 Kari, B. Control of blood glucose levels in alloxan-diabetic rabbits by iontophoresis of insulin. *Diabetes* **35,** 217–221 (1986).
11 Rendell, M. Advances in diabetes for the millennium, drug therapy of type 2 diabetes. *MedGenMed* **6,** 9–11 (2004).
12 Zhuang, J., Wu, H., Yang, Y. & Cao, Y. C. Controlling colloidal superparticle growth through solvophobic interactions. *Angew. Chem. Int. Ed.* **47,** 2208–2212 (2008).
13 Manoharan, V. N., Elsesser, M. T. & Pine, D. J. Dense packing and symmetry in small clusters of microspheres. *Science* **301,** 483–487 (2003).
14 Brannon-Peppas, L. Recent advances on the use of biodegradable microparticles and nanoparticles in controlled drug delivery. *Int. J. Pharm.* **116,** 1–9 (1995).
15 Hans, M. L. & Lowman, A. M. Biodegradable nanoparticles for drug delivery and targeting. *Curr. Opin. Solid State Mater Sci.* **6,** 319–327 (2002).
16 Soppimath, K. S., Aminabhavi, T. M., Kulkarni, A. R. & Rudzinski, W. E. Biodegradable polymeric nanoparticles as drug delivery devices. *J. Control. Release* **70,** 1–20 (2001).
17 Ravi Kumar, M. N. V., Sameti, M., Kneuer, C., Lamprecht, A. & Lehr, C. M. in *Encyclopedia of Nanoscience and Nanotechnology* (ed. Nalwa, H. S.) Vol. 10, 1–19 (American Scientific Publishers, California, USA, 2003).
18 Luengo, J., Weiss, B., Schneider, M., Ehlers, A., Stracke, F., König, K., Kostka, K. H., Lehr, C. M. & Schaefer, U. F. Influence of nanoencapsulation on human skin transport of flufenamic acid. *Skin Pharmacol. Physiol.* **19,** 190–197 (2006).
19 Gu, H. & Roy, K. Topical permeation enhancers efficiently deliver polymer micro and nanoparticles to epidermal Langerhans' cells. *J. Drug Del. Sci. Tech.* **14,** 265–273 (2004).
20 Tekko, I. A., Bonner, M. C. & Williams, A. C. An optimized reverse-phase high performance liquid chromatographic method for evaluating percutaneous absorption of glucosamine hydrochloride. *J. Pharm. Biomed. Anal.* **41,** 385–392 (2006).
21 Kanwischer, M., Kim, S. Y., Kim, J. S., Bian, S., Kwon, K. A. & Kim, D. D. Evaluation of the physicochemical stability and skin permeation of glucosamine sulfate. *Drug Dev. Ind. Pharm.* **31,** 91–97 (2005).
22 Murakami, S. & Aoki, N. Bio-based hydrogels prepared by cross-linking of microbial poly(γ-glutamic acid) with various saccharides. *Biomacromolecules* **7,** 2122–2127 (2006).
23 Sun, S. L., Wang, A. Q. & Gao, Y. C. Study on D-glucosamine-zn (II) complexes by IR spectral analysis. *Spectrosc. Spect. Anal.* **25,** 374–376 (2005).
24 Roseman, S. Reflections on glycobiology. *J. Biol. Chem.* **276,** 1527–1542 (2001).
25 Ghosh, S., Blumenthal, H. J., Davidson, E. & Roseman, S. Glucosamine metabolism. V. Enzymatic synthesis of glucosamine 6-phosphate. *J. Biol. Chem.* **235,** 1265–1273 (1960).
26 Coates, J. in *Encyclopedia of Analytical Chemistry* (ed. Meyers, R. A.) 10815–10837 (John Wiley & Sons Ltd, USA, 2000).
27 Chen, S., Pieper, R., Webster, D. C. & Singh, J. Triblock copolymers: synthesis, characterization, and delivery of a model protein. *Int. J. Pharm.* **288,** 207–218 (2005).
28 Ding, X., Rath, P., Angelo, R., Stringfellow, T., Flanders, E., Dinh, S., Gomez-Orellana, I. & Robinson, J. R. Oral Absorption enhancement of cromolyn sodium through noncovalent complexation. *Pharmaceut. Res.* **21,** 2196–2206 (2004).
29 Barth, H. G. & Mays, J. W. *Modern Methods of Polymer Characterization* 1–561 (Wiley-Interscience, USA, 1991).
30 Alidedeoglu, A. H., York, A. W., Rosado, D. A., McCormick, C. L. & Morgan, S. E. Bioconjugation of D-glucuronic acid sodium salt to well-defined primary amine-containing homopolymers and block copolymers. *J. Polym. Sci. A Polym. Chem.* **48,** 3052–3061 (2010).
31 Zhou, Z., Ribeiro, A. A. & Raetz, C. R. H. High-resolution NMR spectroscopy of lipid A molecules containing 4-amino-4-deoxy-L-arabinose and phosphoethanolamine substituents. *J. Biol. Chem.* **275,** 13542–13551 (2000).
32 Veerapandian, M. & Yun, K. S. Synthesis of silver nanoclusters and functionalization with glucosamine for glyconanoparticles. *Syn. React. Inorg. Metal Org. Chem.* **40,** 56–64 (2010).
33 Niesz, K. & Morse, D. E. Sonication-accelerated catalytic synthesis of oxide nanoparticles. *Nano Today* **5,** 99–105 (2010).
34 Mason, T. J. & Lorimer, J. P. *Applied Sonochemistry: Uses of Power Ultrasound in Chemistry and Processing* 53–54 (Wiley-VCH Verlag GmbH, Germany, 2002).
35 Han, I. H., Choi, S. U., Nam, D. Y., Park, Y. M., Kang, M. J., Kang, K. H., Kim, Y. M., Bae, G. H., Oh, I. Y., Park, J. H., Ye, J. S., Choi, Y. B., Kim, D. K., Lee, J. W. & Choi, Y. W. Identification and assessment of permeability enhancing vehicles for transdermal delivery of glucosamine hydrochloride. *Arch. Pharm. Res.* **33,** 293–299 (2010).
36 Klimas, M., Brethour, C. & Bucknell, D. International market trends analysis for the functional foods and natural health products industry in the United States, Australia, the United Kingdom and Japan, George Morris Centre. *Nutri-Net Canada* (2008).

37 Jonathan, O. O. Trans-acidolysis process for the preparation of carbohydrate fatty-acid esters. *U.S. Patent 6,846,916* Jan 25 (2005).
38 Alvarez-Roman, R., Naik, A., Kalia, Y. N., Guy, R. H. & Fessi, H. Enhancement of topical delivery from biodegradable nanoparticles. *Pharm. Res.* **21,** 1818–1825 (2004).
39 Alvarez-Roman, R., Naik, A., Kalia, Y. N., Guy, R. H. & Fessi, H. Skin penetration and distribution of polymeric nanoparticles. *J. Control. Release* **99,** 53–62 (2004).
40 Zhang, W., Gao, J., Zhu, Q., Zhang, M., Ding, X., Wang, X., Hou, X., Fan, W., Ding, B., Wu, X., Wang, X. & Gao, S. Penetration and distribution of PLGA nanoparticles in the human skin treated with microneedles. *Int. J. Pharm.* **402,** 205–212 (2010).
41 Dinsmore, D., Hsu, M. F., Nikolaides, M. G., Marquez, M., Bausch, A. R. & Weitz, D. A. Colloidosomes: Selectively permeable capsules composed of colloidal particles. *Science* **298,** 1006–1009 (2002).
42 Bera, M. K., Sanyal, M. K., Pal, S., Daillant, J., Datta, A., Kulkarni, G. U., Luzet, D. & Konovalov, O. Reversible buckling in monolayer of gold nanoparticles on water surface. *Europhys. Lett.* **78,** 56003 (2007).
43 Lee, D. & Weitz, D. A. Double emulsion-templated nanoparticle colloidosomes with selective permeability. *Adv. Mater.* **20,** 3498–3503 (2008).
44 Shah, J. C., Sadhale, Y. & Chilukuri, D. M. Cubic phase gels as drug delivery systems. *Adv. Drug Deliv. Rev.* **47,** 229–250 (2001).
45 Lara, M. G., Bentley, M. & Collett, J. H. *In vitro* drug release mechanism and drug loading studies of cubic phase gels. *Int. J. Pharm.* **293,** 241–250 (2005).
46 Boyd, B. J., Whittaker, D. V., Khoo, S. M. & Davery, G. Lyotropic liquid crystalline phases formed from glycerate surfactants as sustained release drug delivery systems. *Int. J. Pharm.* **309,** 218–226 (2006).
47 Cevc, G. & Blume, G. Lipid vesicles penetrate into intact skin owing to the transdermal osmotic gradients and hydration force. *Biochim. Biophys. Acta* **1104,** 226–232 (1992).
48 Cevc, G. In *Rational for the Production and Dermal Application of Lipid Vesicles* (eds Falco, O. B., Korting, H. C. & Maibach, H. I.) 82–90 (Springer-Verlag, Berlin, Germany, 1992).
49 Cevc, G., Schätzlein, A. & Blume, G. Transdermal drug carriers: Basic properties, optimization and transfer efficiency in the case of epicutaneously applied peptides. *J. Control. Release* **36,** 3–6 (1995).
50 Cevc, G., Gebauer, D., Stieber, J., Schätzlein, A. & Blume, G. Ultrafexible vesicles, transferosomes, have an extremely low pore penetration resistance and transport therapeutic amounts of insulin across the intact mammalian skin. *Biochim. Biophys. Acta* **1368,** 201–215 (1998).
51 Honeywell-Nguyen, P. L., Gooris, G. S. & Bouwstra, J. A. Quantitative assessment of the transport of elastic and rigid vesicle components and a model drug from these vesicle formulations into human skin *in vivo*. *J. Invest. Dermatol.* **123,** 902–910 (2004).